0026-895X/94/050993-09$03.00/0

MOLECULAR PHARMACOLOGY, 46:993–1001, 1994.

Functional Heterogeneity of Nicotinic Receptors in the Avian Lateral Spiriform Nucleus Detected with Trimethaphan

WILLIAM R. WEAVER, KATHLEEN M. WOLF, and VINCENT A. CHIAPPINELLI

Department of Pharmacological and Physiological Science, Saint Louis University School of Medicine, St. Louis, Missouri 63104

Received May 26, 1994; Accepted August 15, 1994

SUMMARY

We have examined an excitatory response mediated by nicotinic acetylcholine receptors located on the somata and/or dendrites of chick lateral spiriform neurons. On the basis of pharmacological and anatomical studies, these receptors belong to a subgroup of nicotinic receptors termed high affinity nicotine receptors, because they exhibit a high affinity for nicotinic agonists but little or no sensitivity to α- or κ-bungarotoxin. We now report physiological evidence that high affinity nicotine receptors in the lateral spiriform nucleus are heterogeneous. Intracellular recording in brain slices was used to examine the pharmacological characteristics of nicotinic responses in individual lateral spiriform neurons. Nicotinic responses to brief applications of carbachol were inhibited by trimethaphan, dihydro-β-erythroidine, or *d*-tubocurarine. Trimethaphan was unusual, in that a wide range of concentrations (≤50 μM to >500 μM) were required to block this nicotinic response in different neurons. To quantitate the inhibition observed with trimethaphan and dihydro-β-erythroidine, dose-response curves were generated in superfusion studies using a wide range of concentrations of both agonist (3–3000 μM carbachol in the presence of 1 μM atropine and 0.25 μM tetrodotoxin) and antagonists (10–500 μM trimethaphan or 0.1–3 μM dihydro-β-erythroidine). The data yielded an EC_{50} of 25 ± 5 μM for carbachol, with a Hill coefficient of 1.4 ± 0.1 (mean ± standard error; $n = 8$). In the case of dihydro-β-erythroidine, a narrow range of K_i values was obtained (0.09–0.16 μM; $n = 5$). In contrast, K_i values for trimethaphan varied over a 15-fold concentration range (4–66 μM; $n = 17$), demonstrating that trimethaphan showed selectivity for different receptor subtypes found in the lateral spiriform nucleus. For both antagonists, the data indicate a competitive mode of inhibition.

A hallmark of neuronal nicotinic acetylcholine receptors is their structural and physiological heterogeneity (reviewed in Ref. 1). At least 11 different neuronal nicotinic receptor subunits have been cloned (α2-α9 and β2-β4), and *in situ* hybridization studies have shown distinct localizations within the central nervous system for most subunits (2–5). Many functional neuronal nicotinic receptors are believed to be pentamers consisting of multiple copies of one α and one β subunit and containing at least two acetylcholine binding sites associated with the α subunits. However, receptors that contain two different α subunits (α3 and α5 with β4) (6) are also known, as are homo-oligomeric receptors (α7-α9) (2, 3).

Heterologous expression studies in *Xenopus* oocytes demonstrate that receptor subtypes with quite different pharmacological properties can be formed by various neuronal nicotinic receptor subunit combinations (3–5). One subgroup of receptors exhibits a high affinity for nicotine and other agonists and relative insensitivity to blockade by the snake venom neurotoxins α-bungarotoxin and κ-bungarotoxin and the plant alkaloid methyllycaconitine. These receptors, which we refer to as high affinity nicotine receptors, consist of various combinations of α2, α4, β2, β4, and possibly other receptor subunits (4, 7, 8).

Although the exact subunit compositions of most native neuronal nicotinic receptors are unknown, considerable evidence points to the existence of native receptors with properties similar to those of the high affinity nicotine receptors expressed in oocytes. Native high affinity nicotine receptors have been characterized in binding studies with radiolabeled acetylcholine, nicotine, and cytisine (9–12). Immunoprecipitation studies imply that a majority of high affinity nicotine receptors in chick and rat brain are formed from α4 and β2 subunits (8, 12). In chick brain, the α5 subunit is also associated with a portion of these native receptors (6). Based on oocyte expression studies, the α2 and β4 subunits are also likely to be present in some native high affinity nicotine receptors.

Physiological studies on heterologously expressed receptors indicate that high affinity nicotine receptors containing different receptor subunits can be distinguished by their particular affinities for nicotinic agonists and antagonists (4, 5). In acutely cultured rat neurons, Mulle *et al.* (13) identified pharmacological differences between high affinity nicotine receptors located

This work was supported by National Institutes of Health Grant NS17574. W.R.W. was partially supported by National Institutes of Health Predoctoral Training Grant GM08306.

ABBREVIATIONS: DHβE, dihydro-β-erythroidine; DMPP, 1,1-dimethyl-4-phenylpiperazinium; ACSF, artificial cerebrospinal fluid; SPL, lateral spiriform nucleus; GABA, γ-aminobutyric acid.

on somata of medial habenula neurons and those present on interpeduncular neurons. Surprisingly, even though at least five different nicotinic receptor subunits are expressed in each of these brain regions, those investigators found no electrophysiological evidence for the presence of more than one subtype of high affinity nicotine receptor within neurons from a single nucleus (13, 14). Using a brain slice preparation, Mulle *et al.* (13) identified a third, pharmacologically distinct, nicotinic response, which appeared to be due to presynaptic nicotinic receptors located on nerve terminals in the interpeduncular nucleus.

Electrophysiological and pharmacological techniques have also been used to characterize multiple subtypes of nicotinic receptors in long term cultures of hippocampal neurons (15). At least one of these subtypes (type II) exhibits many of the characteristics of a high affinity nicotine receptor, including high affinity for acetylcholine and potent inhibition by DHβE and κ-bungarotoxin. Type II currents are also relatively insensitive to methyllycaconitine and insensitive to α-bungarotoxin.

In the mesencephalic SPL of the chick, an excitatory response is mediated by nicotinic receptors, with a high affinity for nicotine, that are located on the somata and/or dendrites of SPL neurons (16). Essentially all SPL neurons exhibit this postsynaptic nicotinic response, which can be activated by carbachol, DMPP, or nicotine (17). Consistent with their high affinity nicotine nature, these nicotinic responses are not potently inhibited by either α-bungarotoxin or κ-bungarotoxin (16). Autoradiographic localization studies confirm that the SPL contains a very high density of [^{3}H]nicotine binding sites but no detectable binding of these radiolabled snake toxins (18). Nicotinic receptor subunit protein and/or mRNA prominently expressed by 70–90% of SPL neurons include the α2, α5, and β2 subunits, whereas the α4 subunit is detected in only 30% of these cells (19–21). Up to 30% of SPL neurons are immunopositive for α7 or α8 subunits, which are associated with α-bungarotoxin-sensitive nicotinic receptors (19, 21). The α3 subunit has not been detected in the SPL (20), and no data are currently available on the β4 subunit.

Given that mRNA and protein for multiple nicotinic receptor α subunits are present in SPL neurons, we reasoned that several distinct subtypes of high affinity nicotine receptors might be located in this nucleus and that the functional properties of these receptors might therefore be heterogeneous. We now report that the competitive nicotinic receptor antagonist trimethaphan does distinguish between nicotinic receptors expressed on individual SPL neurons. In some cells, trimethaphan is a potent antagonist, whereas in other neurons it is as much as 15-fold less effective. This finding supports the conclusion that neurons within a single brain region can express more than one type of high affinity nicotine receptor, and it indicates that trimethaphan is a useful ligand for studying neuronal nicotinic receptor subtypes.

Materials and Methods

Intracellular recording in brain slices. Electrophysiological procedures used were similar to those previously described in detail (16) and are summarized below with additions. After decapitation, brains from embryonic (18–21 days of incubation) or newly hatched White Leghorn chicks (SPAFAS, Inc., Peoria, IL) were rapidly removed and placed in cold ACSF (126 mM NaCl, 2.5 mM KCl, 2.5 mM $CaCl_2$, 1.3 mM $MgCl_2$, 1.2 mM Na_2PO_4, 25 mM $NaHCO_3$, 11 mM glucose; continuously bubbled with 95% O_2/5% CO_2 to bring the pH to 7.4). The brains were then glued onto a mounting block and resubmerged in cold ACSF, and 400-μm-thick transverse brain sections were cut on a Vibroslice (Campden Instruments). Sections containing the SPL were either placed in a holding chamber in ACSF at room temperature until needed (0–5 hr) or mounted between two nets in a recording chamber, fully submerged in 1 ml of ACSF maintained at 29–30°, and continuously superfused with ACSF at a rate of 2–3 ml/min.

Microelectrodes for intracellular recording were pulled from filamented capillary glass on a P-87 micropipette puller (Sutter Instrument Co.). These electrodes had resistances of 50–120 MΩ when filled with 3 M KCl. After amplification with an Axoclamp-2A (Axon Instruments) in the balanced-bridge current-clamp mode, signals were continuously displayed on an oscilloscope and recorded with a Gould RS3200 chart recorder and a Vetter video cassette instrumentation recorder.

Dose-response data analysis was performed with InPlot (GraphPAD) and Sigmaplot (Jandel) software. Dose-response curves and their associated parameters were generated using Inplot nonlinear regression, sigmoid curve (log scale), curve-fitting routines. K_i values were determined from log-log plots of the dose ratio − 1 versus antagonist concentration at 50% of the maximal response to carbachol (22, 23).

Brief (20-msec) hyperpolarizing current pulses were passed through the microelectrode to monitor cell input resistance. The bridge balance was monitored and adjusted during the delivery of hyperpolarizing current impulses. Within each neuron, membrane potential was brought to a common value (−70 or −80 mV) before each agonist application, so that observed voltage changes could be directly compared within and between neurons.

Drugs were applied either by bath superfusion at fixed concentrations in ACSF or by pressure ejection of a small volume of drug solution from a pipette into the recording chamber upstream from the brain slice. Superfusion solutions were gravity fed and switched by manually controlled valves. Atropine sulfate (1 μM) was always included in the superfusion ACSF (except when muscarinic responses were examined), to block muscarinic receptors. The antagonists DHβE (Merck Sharp & Dohme Research Laboratories), *d*-tubocurarine chloride (Calbiochem), and trimethaphan camsylate (Hoffmann-La Roche) were prepared at known concentrations in separate flasks of ACSF and were superfused for 15–30 min before testing of SPL neuron responses to agonist applications. The agonists carbamylcholine chloride (carbachol) and *dl*-muscarine chloride were applied either by pressure ejection (1–10 μl of a 10 mM solution) or by bath superfusion at known concentrations (3 μM to 3 mM, for 1–6 min). Cadmium chloride (50–100 μM) in ACSF was superfused in some experiments to demonstrate the postsynaptic nature of the observed responses. In all experiments where agonists were applied at a known concentration by superfusion, 0.25 μM tetrodotoxin (Calbiochem) was included in all external solutions to block action potentials triggered by neuronal depolarization and to inhibit synaptic activity, thus simplifying the measurement of neuronal membrane responses. Unless otherwise indicated, all drugs were purchased from Sigma.

Whole-cell recording in cultured neurons. Potential effects of the nicotinic agonist carbachol on $GABA_A$ receptor-mediated chloride currents were examined in dissociated rat hippocampal cell cultures using previously described procedures (24). A U-tube was used to apply GABA (30 μM) and carbachol (300 μM), either alone or mixed together, in the extracellular solution. GABA currents were elicited during whole-cell voltage-clamp recordings at a holding potential of −30 mV. Because GABA currents desensitize at this potential, responses to drug applications were measured at the peak current within 1 sec after the onset of drug application. Only those cells demonstrating at least 80% recovery of the control response to application of GABA after application of either carbachol alone or carbachol combined with GABA were included for analysis. All results were normalized to the control GABA response, for comparison between cells.

Radiolabel binding experiments. Procedures used for measuring inhibition of [^{3}H]nicotine binding to chick mesencephalon/optic lobe

homogenates were as described previously (25). After decapitation, brains from 19–21-day embryonic or newly hatched White Leghorn chicks (SPAFAS, Inc.) were rapidly removed. The brains were then blocked to isolate the mesencephalon (containing the SPL) and optic lobes, by using a razor blade to make transverse cuts rostral and caudal to the optic lobes. Tissue blocks containing the mesencephalon and optic lobes were placed on ice before homogenization.

For inhibition profiles, a fixed concentration of [^{3}H]nicotine (10 nM) was used with varying concentrations of the competing ligands trimethaphan or DHβE. Nonspecific binding was measured in separate tubes with 1 mM carbachol. *l*-[*N-methyl*-^{3}H]Nicotine (64.0 Ci/mmol) was from NEN/DuPont.

Data analysis was performed using InPlot (GraphPAD). The incubation time (20 min) for 10 nM [^{3}H]nicotine was sufficient to allow equilibrium binding (25), and inhibition constants (K_i) were determined from calculated IC_{50} values by the following equation: $K_i = IC_{50}/(1 + [\text{radioligand}]/K_d)$. The K_d value for [^{3}H]nicotine binding to optic lobe homogenates was 3.1 nM (25).

Results

General cell properties. Intracellular recordings in chick brain slices were performed with microelectrodes inserted into neurons within the SPL. Recordings were made from 390 cells (84 of which were of sufficient length to record usable pharmacological data) in 246 brain slices. Average membrane characteristics of these cells were as follows: input resistance, 107 ± 5 MΩ; time constant, 5.6 ± 0.5 msec; capacitance, 53 ± 4 pF (mean ± standard error, $n = 71$).

Nicotinic nature of responses to carbachol. Several agonists, including nicotine, DMPP, and carbachol, have been used to characterize nicotinic responses in the SPL (16, 17). Of these agonists, carbachol is the least likely to produce desensitization and so was chosen for the present study. Because carbachol can also activate muscarinic acetylcholine receptors, we examined SPL neuron responses to bath superfusion of carbachol (10–100 μM) or muscarine (10–50 μM) with and without 1 μM atropine in the superfusion ACSF. Muscarinic responses in these cells were unremarkable (no detectable response in two cells and slight hyperpolarization with 30 or 50 μM muscarine in two cells). However, to be certain that these small muscarinic responses did not contaminate the carbachol data, 1 μM atropine was included in all superfusion solutions in all other experiments. Addition of 1 μM atropine to the superfusion ACSF did not significantly alter nicotinic responses of SPL neurons to carbachol.

We have recently shown that SPL neurons have functional $GABA_A$ receptors that are activated by the spontaneous release of GABA (17). Because some nicotinic ligands also interact with $GABA_A$ receptors (26, 27), we sought to exclude the possibility that a portion of the actions of carbachol might be mediated by $GABA_A$ receptors. We therefore examined the ability of carbachol to alter a well characterized $GABA_A$ receptor-mediated response in cultured rat hippocampal neurons (24). In these neurons, carbachol (300 μM) alone did not activate $GABA_A$ receptors ($n = 5$), nor was the $GABA_A$ receptor-mediated Cl^- current response to 30 μM GABA changed in any way during coexposure of the neurons to 300 μM carbachol ($n = 5$). These quantitative data, along with similar qualitative observations in chick SPL neurons, lead us to conclude that carbachol does not interact with $GABA_A$ receptors.

Initial pharmacological experiments in SPL neurons were performed using bath superfusion of nicotinic antagonists and pressure ejection of a small volume of the nicotinic agonist carbachol. The control response to pressure ejection of carbachol, in the presence of 1 μM atropine, consisted of a marked depolarization and a series of evoked action potentials as threshold was reached (Fig. 1A). This depolarization and increased firing were not affected by the presence of 100 μM $CdCl_2$ ($n = 9$), demonstrating that carbachol directly activates postsynaptic receptors located on SPL neurons. The nicotinic nature of these excitatory responses was confirmed by their complete blockade by 30–50 μM *d*-tubocurarine ($n = 12$), 50–100 μM DHβE ($n = 18$), and 50–500 μM trimethaphan ($n = 40$).

Effects of trimethaphan on responses to pressure ejection of carbachol. In all SPL neurons examined, postsynaptic nicotinic responses were inhibited at similar concentrations of the antagonists *d*-tubocurarine or DHβE. In contrast, SPL neurons exhibited a very broad range of sensitivities to trimethaphan. The records in Fig. 1A are from an SPL neuron in which the response to carbachol was partially reduced by 25 μM trimethaphan and completely blocked by 50 μM trimethaphan. One third of SPL neurons exhibited nicotinic responses that were completely blocked by 50 μM trimethaphan (10 of 32 cells) (Fig. 1B). Nicotinic responses in 19% of SPL neurons were not blocked by 50 μM trimethaphan but were completely inhibited by 200 μM trimethaphan (six of 32 cells). Other cells within the SPL required even higher concentrations (≥500 μM) of trimethaphan for a complete blockade of nicotinic responses. One half of the cells studied (16 of 32 cells) required >200 μM trimethaphan for complete inhibition of their nicotinic responses. This group of cells thus required a 10-fold greater antagonist concentration than did the group of SPL neurons represented in Fig. 1A. In contrast, nicotinic responses in cells within all three groups distinguished by trimethaphan were readily blocked by 30–50 μM *d*-tubocurarine ($n = 12$) (data not shown).

Effects of trimethaphan on responses to superfusion with carbachol. To more accurately quantify the inhibition of nicotinic responses produced by trimethaphan, we next performed a series of experiments using bath superfusions of both agonist and antagonist. First, control applications of several concentrations of carbachol (3 μM to 3 mM, for 1–6 min) were carried out with a 15-min recovery period between agonist applications. The slice was then superfused with increasing concentrations of trimethaphan (10–500 μM). After at least 30 min of exposure to a particular concentration of trimethaphan, nicotinic responses to several concentrations of carbachol were examined in the same neuron (with the appropriate concentration of trimethaphan also included in the agonist solutions). In these studies, tetrodotoxin (0.25 μM) was included in all extracellular solutions to block spontaneous activity and evoked spikes, thus increasing the accuracy of the measurement of nicotinic responses. This method, using known concentrations of all applied drugs, allowed us to determine in each cell a K_i and pA_2 for trimethaphan, for direct comparison between SPL neurons.

The responses of SPL neurons to superfusion with carbachol involved depolarization to a plateau level at lower concentrations and a maximum depolarizing response followed by apparent desensitization at higher concentrations. Control dose-response curves for carbachol are shown for two SPL neurons in Fig. 2. In Fig. 2B, the reproducibility of maximum responses to replicate applications of various concentrations of carbachol

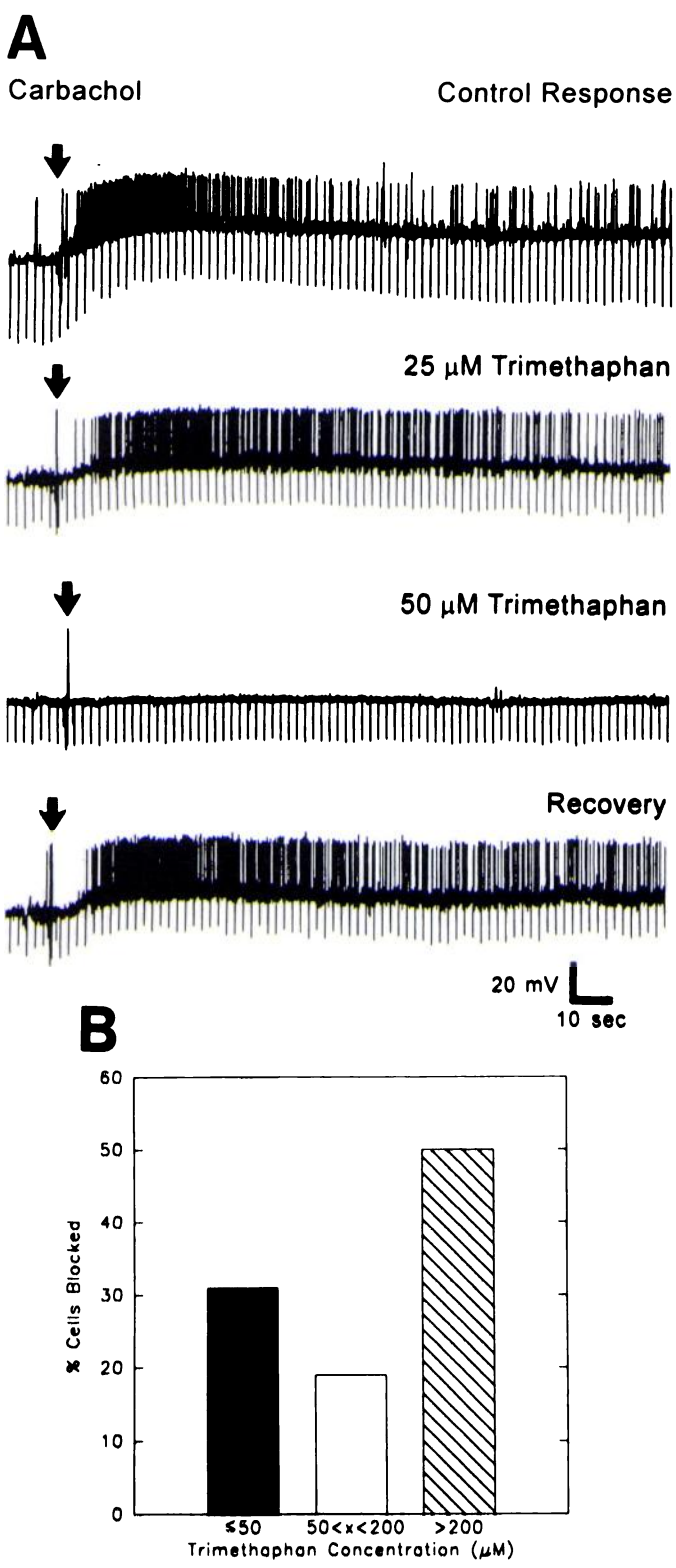

Fig. 1. Requirement for a wide range of trimethaphan concentrations to block nicotinic responses in different SPL neurons. A, Intracellular current-clamp recordings of membrane potentials from an SPL neuron. Carbachol was briefly applied (*arrows*) by pressure ejection (3 μl of a 10 mM solution) into the superfusion flow upstream from the brain slice and produced a depolarization and spiking activity in control ACSF. Trimethaphan was then superfused at fixed concentrations for ≥20 min before agonist applications. Nicotinic responses in the most sensitive SPL neurons were completely blocked by 50 μM trimethaphan. Recovery shown was after 40 min of washing out of trimethaphan. Rapid downward deflections were due to constant hyperpolarizing current pulses of 20-msec duration and were used to assess cell input resistance. In all records, membrane potential was −70 mV before carbachol application. Action potentials are attenuated in this chart record. B, Summary of trimethaphan inhibition of SPL neuron responses to pressure ejection of carbachol. Data from 32 SPL neurons are grouped into three categories; in 31% of neurons the nicotinic responses were completely inhibited by 50 μM trimethaphan (n = 10), in 19% of cells 200 μM trimethaphan was required (n = 6), and in 50% of neurons >200 μM trimethaphan was required for complete blockade of the response to carbachol (n = 16).

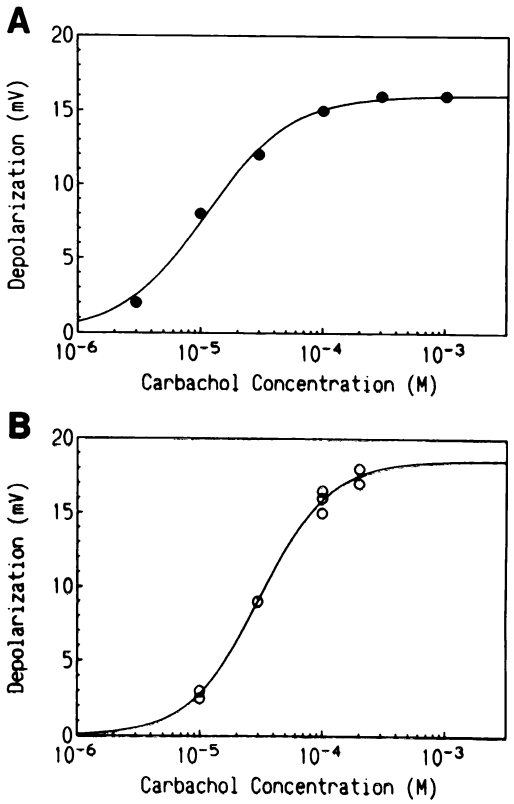

Fig. 2. Dose-response curves recorded in SPL neurons using bath superfusion with carbachol. A, Carbachol was applied by bath superfusion (1–5 min; each agonist superfusion was separated by ≥10 min) over a wide concentration range (3–1000 μM), and the maximum depolarization produced was recorded in an SPL neuron. The sigmoid-shaped response begins to plateau at 100 μM. The InPlot-generated curve shown yields a Hill slope of 1.3, EC_{50} of 11 μM, and r^2 value of 0.994. B, Responses to replicate agonist applications at various carbachol concentrations in another SPL neuron are shown (10 μM carbachol, n = 3; 30 μM, n = 3; 100 μM, n = 4; 200 μM, n = 2).

is illustrated (n = 2–4) (fitted-curve values for these dose-response data were EC_{50} = 31 μM, Hill slope = 1.5, and r^2 = 1.000).

A typical control response to superfusion with 30 μM carbachol and inhibition of this depolarization by increasing concentrations of trimethaphan are illustrated for an SPL neuron in Fig. 3A. Fig. 3B shows the effects of different concentrations of trimethaphan on the response of this neuron to carbachol. Increasing concentrations of trimethaphan (10–200 μM) produced a rightward shift of the carbachol dose-response curve. Recovery of responses to carbachol after the final washout of trimethaphan can be seen in the leftmost curve (fitted-curve values for control and recovery responses were EC_{50} = 41 μM and 25 μM, Hill slope = 1.4 and 1.4, and r^2 = 1.000 and 0.990, respectively). The plot of the dose ratio − 1 versus trimetha-

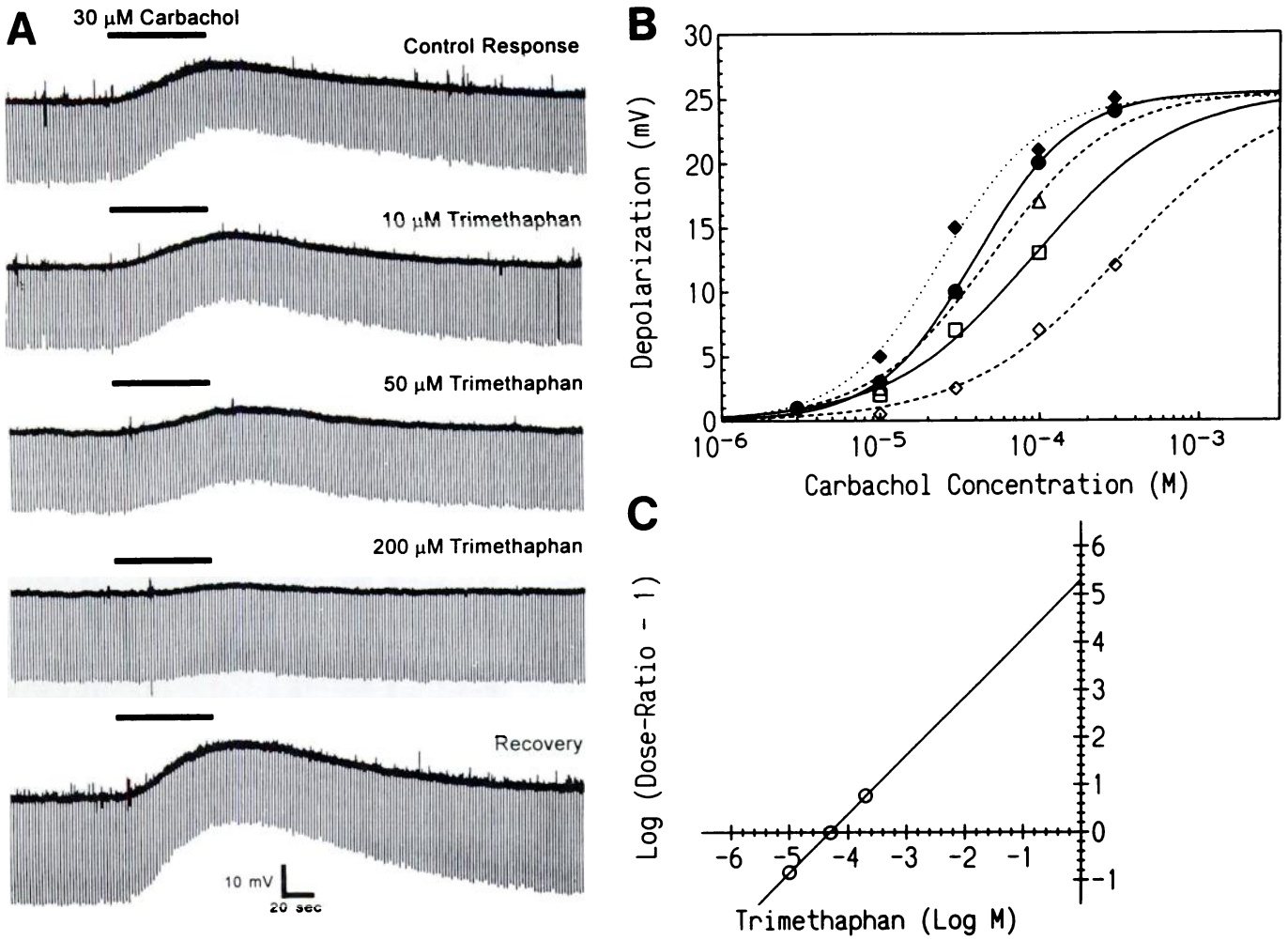

Fig. 3. Trimethaphan inhibition of nicotinic responses to carbachol superfusion. A, Membrane potential response to superfusion with 30 μM carbachol (1 min) (*solid bars above records*) is shown for an SPL neuron under control conditions and in the presence of various concentrations of trimethaphan. Tetrodotoxin (0.25 μM), present in all external solutions, was used to block spiking activity and spontaneous events. B, Dose-response curves generated for carbachol (3–300 μM), in the same SPL neuron as shown in A, under control conditions and in the presence of various concentrations of trimethaphan are shown. ●, Control responses; △, 10 μM trimethaphan; □, 50 μM trimethaphan; ◇, 200 μM trimethaphan; ♦, recovery (obtained after all trimethaphan was washed out for ≥23 min). C, The data in B were used to prepare a log-log plot of the dose ratio − 1 versus trimethaphan concentration at 10 μM, 50 μM, and 200 μM trimethaphan (slope = 1.21 ± 0.09, ± standard error; dose ratio was determined at 50% of the maximal response to carbachol). In this SPL neuron, the K_i for trimethaphan, equivalent to the *x*-axis intercept, was 53 μM.

phan concentration for the calculation of the K_i (53 μM) for this cell is presented in Fig. 3C.

Similar to our experiments using pressure ejections of agonist, different cells within the SPL exhibited markedly different sensitivities to trimethaphan inhibition of nicotinic responses elicited by carbachol superfusion. Inhibitory constants (K_i) for trimethaphan in SPL neurons ranged from 4 to 66 μM (n = 17), with a significant number of cells throughout this concentration range (see Fig. 6). Although there was some variability from neuron to neuron in the maximum depolarization in response to carbachol (18 ± 1 mV, mean ± standard error; range, 11–24 mV; n = 17), there was no significant correlation of the K_i determined for trimethaphan with the maximum depolarization obtained in the cells (Fig. 4) (r^2 = 0.140).

Effects of DHβE on responses to superfusion with carbachol. To demonstrate that the heterogeneous results obtained with trimethaphan were not due to inherent variability in the experimental protocol, we next performed a series of experiments on SPL neurons using DHβE as the nicotinic

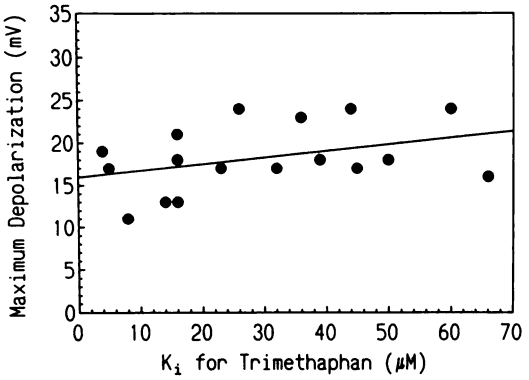

Fig. 4. Lack of correlation between K_i for trimethaphan and maximum depolarization in response to carbachol. Data are shown for the 17 SPL neurons in which the K_i for trimethaphan was determined. The slope of the linear least-squares regression line drawn is not significantly different from 0 (r^2 = 0.140).

antagonist. As with the previous study, varying concentrations of carbachol (3 μM to 30 mM) were applied by superfusion, with and without multiple concentrations of DHβE (0.1–3 μM). A set of dose-response curves for carbachol and inhibition of the response by DHβE are presented in Fig. 5A. Increasing concentrations of DHβE shifted the curve to the right in a parallel manner, and increasing concentrations of carbachol could overcome the inhibition by DHβE and return responses to maximal control levels (Fig. 5A). The plot of dose ratio − 1 versus antagonist concentration (Fig. 5B) allowed calculation of the K_i for this cell (0.16 μM). The competitive nature of DHβE antagonism can also be seen in the slope of this plot (1.05).

In sharp contrast to the trimethaphan results, the range of K_i values obtained for inhibition by DHβE was very narrow (0.09–0.16 μM, $n = 5$). The highest K_i observed for DHβE inhibition (0.16 μM) was less than twice the lowest value (0.09 μM), whereas the highest value for trimethaphan inhibition (66 μM) was >15 times the smallest (4 μM). A comparison of the inhibitory constants for these two antagonists in different SPL cells is presented graphically in Fig. 6.

Inhibition of [^{3}H]nicotine binding. On the basis of previous electrophysiological, pharmacological, and autoradiographic studies (16, 18), functional nicotinic receptors in the SPL appear to be identical to sites recognized with high affinity (K_d = 3.1 nM) (25) by [^{3}H]nicotine in this nucleus. We therefore carried out radioligand binding experiments to measure the ability of trimethaphan and DHβE to inhibit specific [^{3}H] nicotine binding to homogenates of chick mesencephalon/optic lobe. In this assay, trimethaphan (K_i = 390 μM) was >100-fold less potent than DHβE (K_i = 3.0 μM). There was no indication of multiple affinities or positive or negative cooperativity for either antagonist, because the calculated Hill slopes were 0.96–1.02 (Fig. 7). The K_i obtained for carbachol against [^{3}H]nicotine binding in chick brain was 0.48 μM.

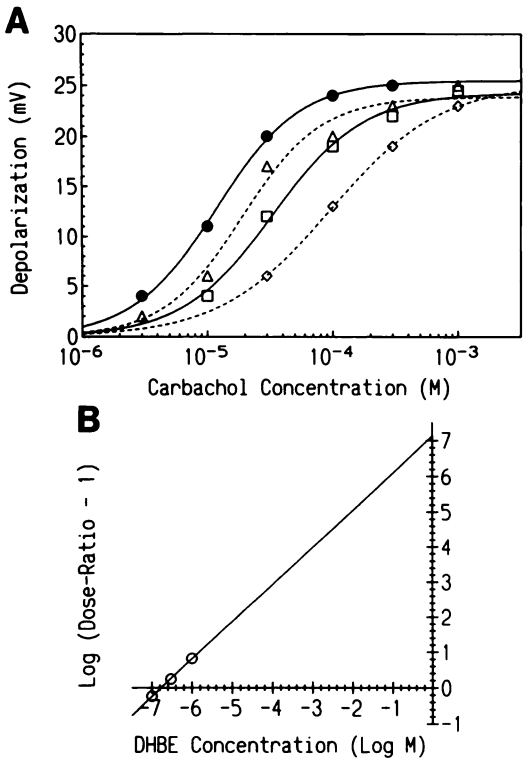

Fig. 5. DHβE inhibition of nicotinic responses to carbachol superfusion, recorded in an SPL neuron. A, Dose-response curves for carbachol superfusions (3–1000 μM) under control conditions and in the presence of various concentrations of DHβE are shown. ●, Control responses; △, 0.1 μM DHβE; □, 0.3 μM DHβE; ◇, 1 μM DHβE. B, The data in A were used to prepare a log-log plot of the dose ratio − 1 versus DHβE concentration at 0.1 μM, 0.3 μM, and 1 μM DHβE (slope = 1.05 ± 0.03, ± standard error; dose ratio was determined at 50% of the maximal response to carbachol). The K_i determined for this SPL neuron (x-axis intercept) was 0.16 μM.

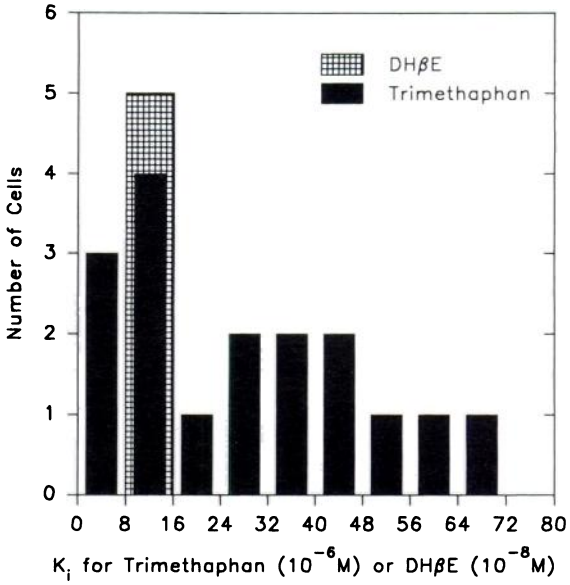

Fig. 6. Summary of data for trimethaphan and DHβE inhibition of nicotinic responses to carbachol superfusions in SPL neurons. All K_i values determined for trimethaphan and DHβE inhibition of nicotinic responses in SPL neurons are plotted on the same scale for ease in comparing the heterogeneity of the trimethaphan values with the narrower range of DHβE values obtained. For trimethaphan (n = 17), the scale is 0 to 80 × 10^{-6} M; for DHβE (n = 5), the scale is 0 to 80 × 10^{-8} M.

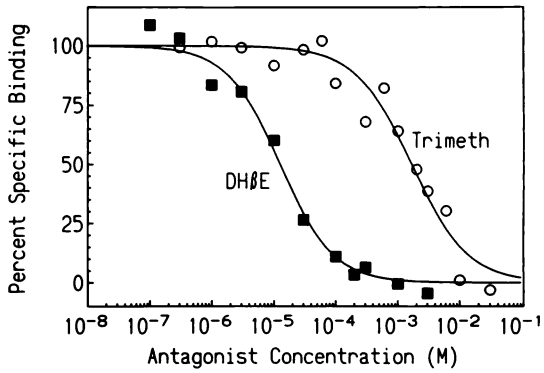

Fig. 7. Trimethaphan and DHβE inhibition of [^{3}H]nicotine binding to chick mesencephalon/optic lobe homogenates. The graph shows inhibition curves generated for trimethaphan (*Trimeth*) and DHβE against 10 nM [^{3}H]nicotine binding over a wide range of antagonist concentrations. *Points*, average values obtained from two separate experiments for each antagonist. *Curves* (generated by InPlot) yielded the following values: for trimethaphan, K_i = 390 μM and Hill coefficient = 0.96; for DHβE, K_i = 3.0 μM and Hill coefficient = 1.02.

Discussion

Trimethapan exhibits selectivity for SPL neuron nicotinic receptor subtypes. The present results demonstrate that the antagonist trimethaphan has a wide range of potencies against functional nicotinic receptors in the chick SPL. There

is as much as a 15-fold difference in the K_i values determined for trimethaphan in separate neurons within this nucleus. In contrast, K_i values for DHβE, obtained in an identical fashion, differ by only 2-fold among all SPL neurons examined. The results indicate that high affinity nicotine receptors located on SPL neurons are not homogeneous.

Pharmacological properties of nicotinic receptors in the SPL. Functional studies have identified two types of nicotinic responses in the chick SPL. One response, a marked enhancement of GABAergic spontaneous currents, is likely to be due to nicotinic receptors located in a "preterminal" or presynaptic position on GABAergic nerve terminals within the SPL (17). The second nicotinic response is a large sustained inward current (in whole-cell voltage-clamp recordings) or depolarization (in intracellular current-clamp recordings) that is mediated by nicotinic receptors located directly on the cell somata and/or dendrites of SPL neurons (the present study and Refs. 16 and 17). It is specifically these somatic/dendritic postsynaptic nicotinic receptors that have been characterized in the present study.

Certain pharmacological properties of somatic/dendritic SPL nicotinic receptors have been described. These receptors are inhibited by *d*-tubocurarine and DHβE but are insensitive to blockade by either κ- or α-bungarotoxin (16). They are activated by nicotine, carbachol, and DMPP (17). Methyllycaconitine, an extremely potent antagonist at neuronal α-bungarotoxin-sensitive receptors ($IC_{50} < 1$ nM) (15, 28), is much less effective at SPL nicotinic receptors ($IC_{50} = 10$ μM).[1] All of these pharmacological characteristics are consistent with receptors belonging to the high affinity nicotine subgroup of neuronal nicotinic receptors. Autoradiographic studies confirm that the SPL contains a very high density of [^{3}H]nicotine sites, whereas radiolabeled snake neurotoxin sites are not detected in this brain region (18).

Interactions of DHβE with nicotinic receptors in the SPL. In the present study, we determined that DHβE is a potent antagonist of depolarizing responses mediated by somatic/dendritic SPL nicotinic receptors, with a narrow K_i range of 0.09–0.16 μM. The parallel rightward shifts in carbachol dose-response curves produced by DHβE and the unitary pA_2 plot slopes are evidence for a competitive mechanism of receptor blockade, a finding that agrees with a previous study that examined DHβE action on invertebrate central nicotinic receptors (29). DHβE was also very potent in inhibiting [^{3}H]nicotine binding to homogenates of chick mesencephalon/optic lobe (K_i = 3.0 μM), a finding that is consistent with the antagonist acting directly at or near the agonist binding site of the receptor.

Comparison of DHβE effects in SPL neurons and at other neuronal nicotinic receptors. Similar to our findings in the SPL, other investigators have reported that DHβE is a potent antagonist in functional assays of high affinity nicotine receptors on cultured hippocampal neurons ($IC_{50} < 10$ nM) (15) and with the $\alpha4\beta2$ subunit combination expressed in oocytes ($IC_{50} = 4$ nM) (30). In acutely dissociated rat central neurons, IC_{50} values of 2 μM and 30 μM have been reported for DHβE inhibition of responses mediated by high affinity nicotine receptors on interpeduncular and medial habenular neurons, respectively (13). Even though IC_{50} and K_i values are not directly comparable, the data suggest that the high affinity nicotine receptors in the SPL more closely resemble those in the interpeduncular nucleus than those in the medial habenula. Interestingly, the $\alpha2$ and $\alpha5$ subunits, which are both prominently expressed in SPL neurons (19, 20), are also found in the interpeduncular nucleus but not in the medial habenula (13). All three brain regions contain $\alpha4$ and $\beta2$ subunits (13, 20).

Our K_i value of 3.0 μM for DHβE in the [^{3}H]nicotine binding assay is similar to that previously obtained for DHβE against [^{3}H]acetylcholine binding to chick brain homogenates (K_i = 1.2 μM) (9). DHβE is among the most potent nicotinic antagonists at inhibiting [^{3}H]nicotine binding to rat brain (K_i = 0.09–1.3 μM) (11, 31) and striatum (IC_{50} = 0.24–0.47 μM) (32).

For both DHβE and trimethaphan, potencies in the physiological assay were approximately 20-fold higher than corresponding potencies in the binding assay. This discrepancy is likely due to the fact that functional assays measure antagonist potency at a different conformational state of the receptor than do binding assays. Agonists exhibit two distinct binding affinities for nicotinic receptors. The low affinity agonist state is associated with activated receptors, whereas in the high affinity agonist state the receptors are desensitized (33, 34). The functional assay thus measures antagonist potency against low affinity agonist binding. In contrast, the binding assay, in which the receptor is exposed to the agonist for sufficient time to shift the receptor conformation toward the high affinity agonist state, measures antagonist competition at the desensitized state of the receptor. For example, the agonist carbachol had an EC_{50} of 25 μM in the SPL physiological assay but a much higher potency (K_i = 0.48 μM) in the chick mesencephalon/optic lobe binding assay. Our results with both DHβE and trimethaphan are consistent with a competitive mechanism of inhibition, because lower concentrations of the antagonists were required to compete against agonist binding in the physiological assay, compared with the binding assay.

Interactions of trimethaphan with nicotinic receptors in the SPL. Trimethaphan inhibited responses of SPL neurons to carbachol superfusions with a wide range of K_i values, from 4 to 66 μM. The 15-fold variation in K_i values observed in the superfusion studies was consistent with the >10-fold range of concentrations of trimethaphan (≤50 to >500 μM) required to block depolarizing responses to pressure ejections of carbachol on SPL neurons. Thus, trimethaphan, but not DHβE, appeared to exhibit multiple affinities for high affinity nicotine receptors in the SPL.

Several observations support a competitive mechanism of antagonism by trimethaphan at SPL neuronal nicotinic receptors; 1) the blockade is reversible, 2) the slopes of the dose ratio − 1 versus trimethaphan concentration plots are near unity (0.95 ± 0.10, mean ± standard error, n = 14 neurons), and 3) inhibition by up to 50 μM trimethaphan can be overcome by increasing concentrations of carbachol, returning SPL responses to control levels (data not shown). Trimethaphan is also a competitive antagonist at other neuronal nicotinic receptors (35–37). We cannot rule out an additional noncompetitive component to the actions of trimethaphan at higher concentrations (>200 μM). Observed deviations from ideal competitive dose-response curves at high antagonist concentrations could be due to such effects or could be primarily the result of the more rapid desensitization seen at the high agonist concentrations required to compete with antagonist, an effect also observed at high concentrations of DHβE. Finally, because tri-

[1] L. Yum, K. M. Wolf, and V. A. Chiappinelli, unpublished observations.

methaphan selects between nicotinic receptor subtypes, multiple receptor subtypes on a single SPL neuron may result in nonideal dose-response curves.

Trimethaphan inhibited the binding of [^{3}H]nicotine to chick mesencephalon/optic lobe homogenates with a K_i of 390 μM. Thus, for both binding and functional assays of high affinity nicotine receptors, trimethaphan was an approximately 100-fold less potent antagonist than DHβE. We are unsure why we did not detect evidence of heterogeneity in the binding of trimethaphan to [^{3}H]nicotine sites. The physiological results suggest a possible range of affinities of only 10–15-fold, which would make separation of two or more sites difficult in the binding competition assay. Furthermore, as mentioned above, the binding assay is not directly comparable to the functional assay because the binding assay measures desensitized receptors, whereas the functional assay detects the low affinity agonist state of the receptor.

Comparison of trimethaphan effects in SPL neurons and at other neuronal nicotinic receptors. Trimethaphan is a relatively weak antagonist in SPL neurons, with a K_i range of 4–66 μM for functional nicotinic receptors and a K_i of 390 μM against [^{3}H]nicotine binding in chick mesencephalon/optic lobe homogenates. Although a previous study confirms that trimethaphan is a weak inhibitor of [^{3}H]nicotine binding in brain (K_i = 620 μM for rat cerebral cortex) (38), the present report is the first to demonstrate its comparatively low potency in a physiological assay for high affinity nicotine receptors. In contrast, trimethaphan exhibits considerably higher affinity for κ-bungarotoxin-sensitive nicotinic receptors than for the κ-bungarotoxin-insensitive receptors in the SPL. For example, trimethaphan blocks κ-bungarotoxin-sensitive nicotinic receptors in autonomic ganglia with IC_{50} values of 0.3–25 μM (35, 36, 39) and inhibits ^{125}I-κ-bungarotoxin binding to chick ciliary ganglion and retina with K_i values of 9.3 μM and 1.1 μM, respectively (40, 41). The data also indicate that trimethaphan may be up to 10-fold more potent at blocking sympathetic nicotinic receptors than those found in parasympathetic ganglia (35, 39). It is intriguing that trimethaphan may thus subdivide both high affinity nicotine receptors and κ-bungarotoxin-sensitive nicotinic receptors.

Subpopulations of neurons within the SPL. Our results indicate that, within the SPL, there exist subpopulations of neurons that can be distinguished on the basis of the trimethaphan sensitivity of nicotinic receptors on the surface of these neurons. Although it is possible that each SPL neuron expresses only a single functional subtype of receptor, it is more likely that many SPL neurons have two or more subtypes of somatic/dendritic nicotinic receptors. The functional evidence for this multiplicity of receptors is 2-fold. First, our K_i values for trimethaphan were spread over the entire 15-fold range obtained, consistent with individual neurons expressing varied ratios of receptor subtypes having different sensitivities to trimethaphan. Second, single-channel studies in progress in our laboratory indicate that individual SPL neurons can exhibit more than one type of nicotinic receptor channel.[2] Thus, individual SPL neurons express multiple subtypes of functional nicotinic receptors, as previously reported for autonomic ganglion neurons (42, 43) and cultured hippocampal neurons (15).

The expression of multiple nicotinic receptor subunits (α2, α4, α5, and β2) (19–21) in individual SPL neurons provides the structural basis for the functional heterogeneity that we have identified. Although the actual subunit compositions of native receptors are extremely difficult to determine, particularly when two or more receptor subunits and heterogeneity are present, it may be useful to examine the potency of trimethaphan for blocking the function of nicotinic receptors consisting of various known subunit combinations in heterologous expression studies.

Trimethaphan sensitivity of nicotinic responses in particular SPL neurons did not correlate well with such general cell characteristics as input resistance, capacitance, or time constant (data not shown). There was also no apparent correlation of trimethaphan sensitivity with the EC_{50} for carbachol in the neuron, the depth of the cell within the slice, the location of the cell within the SPL, the electrode resistance, the presence or absence of inward rectification, or as a function of a particular brain slice (i.e., cells within the same brain slice often required substantially different concentrations of trimethaphan for a comparable level of inhibition). Thus, at present the only property of which we are aware that distinguishes these neuronal subpopulations within the SPL is sensitivity to trimethaphan. Neurons in the SPL are all GABAergic, and all also contain enkephalin (44). Both GABAergic and cholinergic inputs have been identified in the SPL, where they appear to have a wide distribution (17, 44, 45). Because there are no known interneurons in the SPL, the available evidence indicates that all of the cells from which we recorded are GABAergic/enkephalinergic neurons that receive GABAergic and cholinergic innervation. Presumably, the somatic/dendritic high affinity nicotine receptors on these neurons respond to acetylcholine released from cholinergic fibers entering the SPL, and activation of these receptors would be expected to enhance the activity of SPL neurons.

The present results are the first to demonstrate that, within neurons in a single brain region, more than one type of high affinity nicotine receptor can be detected using intracellular recording. The results thus extend previous observations of heterogeneity among neuronal nicotinic receptors. The possible functional role of such receptor heterogeneity remains to be explained. Single-channel studies currently in progress in our laboratory demonstrate that the properties of single nicotinic receptor channels on the somata of SPL neurons are not homogeneous and that a single SPL neuron can express more than one subtype of nicotinic channel. These studies may help to clarify the functional differences between subtypes of high affinity nicotine receptors in the brain.

Acknowledgments

We are grateful to Drs. Terrance M. Egan and Kong-Woo Yoon for helpful suggestions during the course of these experiments. We would like to thank Virginia E. Wotring and Dr. Yoon for assistance in carrying out the physiological experiments on cultured hippocampal neurons. We thank Hoffmann-La Roche, Inc., for providing trimethaphan and Merck Sharp & Dohme Research Laboratories for providing DHβE.

References

1. Sargent, P. B. The diversity of neuronal nicotinic acetylcholine receptors. *Annu. Rev. Neurosci.* **16**:403–443 (1993).
2. Elgoyhen, A. B., D. Johnson, J. Boulter, D. Vetter, and S. F. Heinemann. Cloning and functional expression of α9: a novel acetylcholine-gated ion channel, in *International Symposium on Nicotine: The Effects of Nicotine on Biological Systems II: The Abstracts* (P. B. S. Clarke, M. Quik, K. Thurau, and F. Adlkofer, eds.). Birkhauser, Basel, P7 (1994).
3. Couturier, S., D. Bertrand, J.-M. Matter, M.-C. Hernandez, S. Bertrand, N. Miller, S. Valera, T. Barkas, and M. Ballivet. A neuronal nicotinic acetylcho-

[2] W. R. Weaver and V. A. Chiappinelli, unpublished observations.

line receptor subunit (α7) is developmentally regulated and forms a homo-oligomeric channel blocked by α-BTX. *Neuron* **5**:847–856 (1990).
4. Luetje, C. W., K. Wada, S. Rogers, S. N. Abramson, K. Tsuji, S. Heinemann, and J. Patrick. Neurotoxins distinguish between different neuronal nicotinic acetylcholine receptor subunit combinations. *J. Neurochem.* **55**:632–640 (1990).
5. Luetje, C. W., and J. Patrick. Both α- and β-subunits contribute to the agonist sensitivity of neuronal nicotinic acetylcholine receptors. *J. Neurosci.* **11**:837–845 (1991).
6. Conroy, W. G., A. B. Vernallis, and D. K. Berg. The α5 gene product assembles with multiple acetylcholine receptor subunits to form distinctive receptor subtypes in brain. *Neuron* **9**:679–691 (1992).
7. Bertrand, D., M. Ballivet, and D. Rungger. Activation and blocking of neuronal nicotinic acetylcholine receptor reconstituted in *Xenopus* oocytes. *Proc. Natl. Acad. Sci. USA* **87**:1993–1997 (1990).
8. Whiting, P., R. Schoepfer, J. Lindstrom, and T. Priestley. Structural and pharmacological characterization of the major brain nicotinic acetylcholine receptor subtype stably expressed in mouse fibroblasts. *Mol. Pharmacol.* **40**:463–472 (1991).
9. Schneider, M., C. Adee, H. Betz, and J. Schmidt. Biochemical characterization of two nicotinic receptors from the optic lobe of the chick. *J. Biol. Chem.* **260**:14505–14512 (1985).
10. Whiting, P., and J. Lindstrom. Pharmacological properties of immunoisolated neuronal nicotinic receptors. *J. Neurosci.* **6**:3061–3069 (1986).
11. Martino-Barrows, A. M., and K. J. Kellar. [^{3}H]Acetylcholine and [^{3}H](−)nicotine label the same recognition site in rat brain. *Mol. Pharmacol.* **31**:169–174 (1987).
12. Flores, C. M., S. W. Rogers, L. A. Pabreza, B. B. Wolfe, and K. J. Kellar. A subtype of nicotinic cholinergic receptor in rat brain is composed of α4 and β2 subunits and is up-regulated by chronic nicotine treatment. *Mol. Pharmacol.* **41**:31–37 (1992).
13. Mulle, C., C. Vidal, P. Benoit, and J.-P. Changeux. Existence of different subtypes of nicotinic acetylcholine receptors in the rat habenulo-interpeduncular system. *J. Neurosci.* **11**:2588–2597 (1991).
14. Mulle, C., and J.-P. Changeux. A novel type of nicotinic receptor in the rat central nervous system characterized by patch-clamp techniques. *J. Neurosci.* **10**:169–175 (1990).
15. Alkondon, M., and E. X. Albuquerque. Diversity of nicotinic acetylcholine receptors in rat hippocampal neurons. I. Pharmacological and functional evidence for distinct structural subtypes. *J. Pharmacol. Exp. Ther.* **265**:1455–1473 (1993).
16. Sorenson, E. M., and V. A. Chiappinelli. Intracellular recording in avian brain of a nicotinic response that is insensitive to κ-bungarotoxin. *Neuron* **5**:307–315 (1990).
17. McMahon, L. L., K.-W. Yoon, and V. A. Chiappinelli. Nicotinic receptor activation facilitates GABAergic neurotransmission in the avian lateral spiriform nucleus. *Neuroscience* **59**:689–698 (1994).
18. Sorenson, E. M., and V. A. Chiappinelli. Localization of ^{3}H-nicotine, ^{125}I-κ-bungarotoxin and ^{125}I-α-bungarotoxin binding to nicotinic sites in the chicken forebrain and midbrain. *J. Comp. Neurol.* **323**:1–12 (1992).
19. Ullian, E. M., and P. B. Sargent. Cellular diversity in the expression of nicotinic acetylcholine receptor subunits in the chick central nervous system, in *International Symposium on Nicotine: The Effects of Nicotine on Biological Systems II: The Abstracts* (P. B. S. Clarke, M. Quik, K. Thurau, and F. Adlkofer, eds.). Birkhauser, Basel, P3 (1994).
20. Morris, B. J., A. A. Hicks, W. Wisden, M. G. Darlison, S. P. Hunt, and E. A. Barnard. Distinct regional expression of nicotinic acetylcholine receptor genes in chick brain. *Mol. Brain Res.* **7**:305–315 (1990).
21. Britto, L. R. G., K. T. Keyser, J. M. Lindstrom, and H. J. Karten. Immunohistochemical localization of nicotinic acetylcholine receptor subunits in the mesencephalon and diencephalon of the chick (*Gallus gallus*). *J. Comp. Neurol.* **317**:325–340 (1992).
22. Schild, H. O. pA, a new scale for the measurement of drug antagonism. *Br. J. Pharmacol.* **2**:189–206 (1947).
23. Tallarida, R. J., and L. S. Jacob. *The Dose-Response Relation in Pharmacology*. Springer-Verlag, New York (1979).
24. Yoon, K.-W., D. F. Covey, and S. M. Rothman. Multiple mechanisms of picrotoxin block of GABA-induced currents in rat hippocampal neurons. *J. Physiol. (Lond.)* **464**:423–439 (1993).
25. Wolf, K. M., A. Ciarleglio, and V. A. Chiappinelli. κ-Bungarotoxin: binding of a neuronal nicotinic receptor antagonist to chick optic lobe and skeletal muscle. *Brain Res.* **439**:249–258 (1988).
26. Lebeda, F. J., J. J. Hablitz, and D. Johnston. Antagonism of GABA-mediated responses by *d*-tubocurarine in hippocampal neurons. *J. Neurophysiol.* **48**:622–633 (1982).
27. Wotring, V. E., and K.-W. Yoon. Actions of nicotinic antagonists at the $GABA_A$ receptor. *Soc. Neurosci. Abstr.* **19**:1137 (1993).
28. Alkondon, M., E. F. R. Pereira, S. Wonnacott, and E. X. Albuquerque. Blockade of nicotinic currents in hippocampal neurons defines methyllycaconitine as a potent and specific receptor antagonist. *Mol. Pharmacol.* **41**:802–808 (1992).
29. David, J. A., and D. B. Sattelle. Actions of cholinergic pharmacological agents on the cell body membrane of the fast coxal depressor motoneurone of the cockroach (*Periplaneta americana*). *J. Exp. Biol.* **108**:119–136 (1984).
30. Luetje, C. W., J. Patrick, and P. Séguéla. Nicotine receptors in the mammalian brain. *FASEB J.* **4**:2753–2760 (1990).
31. Rapier, C., G. G. Lunt, and S. Wonnacott. Nicotinic modulation of [^{3}H] dopamine release from striatal synaptosomes: pharmacological characterisation. *J. Neurochem.* **54**:937–945 (1990).
32. Clarke, P. B. S., C. B. Pert, and A. Pert. Autoradiographic distribution of nicotine receptors in rat brain. *Brain Res.* **323**:390–395 (1984).
33. Stroud, R. M., M. P. McCarthy, and M. Shuster. Nicotinic acetylcholine receptor superfamily of ligand-gated ion channels. *Biochemistry* **29**:11009–11010 (1990).
34. Wonnacott, S. Brain nicotine binding sites. *Hum. Toxicol.* **6**:343–353 (1987).
35. van Rossum, J. M. Classification and molecular pharmacology of ganglionic blocking agents. II. Mode of action of competitive and non-competitive ganglionic blocking agents. *Int. J. Neuropharmacol.* **1**:403–421 (1962).
36. Rang, H. P. The action of ganglionic blocking drugs on the synaptic responses of rat submandibular ganglion cells. *Br. J. Pharmacol.* **75**:151–168 (1982).
37. Chiappinelli, V. A. κ-Neurotoxins and α-neurotoxins: effects on neuronal nicotinic acetylcholine receptors, in *Snake Toxins* (A. L. Harvey, ed.). Pergamon Press, New York, 223–258 (1991).
38. Loiacono, R., J. Stephenson, and F. Mitchelson. Multiple binding sites for nicotine receptor antagonists in inhibiting [^{3}H](−)-nicotine binding in rat cortex. *Neuropharmacology* **32**:847–853 (1993).
39. Pinnock, R. D., S. C. R. Lummis, V. A. Chiappinelli, and D. B. Sattelle. κ-Bungarotoxin blocks an α-bungarotoxin-sensitive nicotinic receptor in the insect central nervous system. *Brain Res.* **458**:45–52 (1988).
40. Halvorsen, S. W., and D. K. Berg. Identification of a nicotinic acetylcholine receptor on neurons using an α-neurotoxin that blocks receptor function. *J. Neurosci.* **6**:3405–3412 (1986).
41. Loring, R. H., E. Aizenman, S. A. Lipton, and R. E. Zigmond. Characterization of nicotinic receptors in chick retina using a snake venom neurotoxin that blocks neuronal nicotinic receptor function. *J. Neurosci.* **9**:2423–2431 (1989).
42. Moss, B. L., and L. W. Role. Enhanced ACh sensitivity is accompanied by changes in ACh receptor channel properties and segregation of ACh receptor subtypes on sympathetic neurons during innervation *in vivo*. *J. Neurosci.* **13**:13–28 (1993).
43. Zhang, Z.-W., S. Vijayaraghavan, and D. K. Berg. Neuronal acetylcholine receptors that bind α-bungarotoxin with high affinity function as ligand-gated ion channels. *Neuron* **12**:167–177 (1994).
44. Veenman, C. L., and A. Reiner. The distribution of GABA-containing perikarya, fibers, and terminals in the forebrain and midbrain of pigeons, with particular reference to the basal ganglia and its projection targets. *J. Comp. Neurol.* **339**:209–250 (1994).
45. Sorenson, E. M., D. Parkinson, J. L. Dahl, and V. A. Chiappinelli. Immunohistochemical localization of choline acetyltransferase in the chicken mesencephalon. *J. Comp. Neurol.* **281**:641–657 (1989).

Send reprint requests to: Vincent A. Chiappinelli, Department of Pharmacological and Physiological Science, Saint Louis University School of Medicine, 1402 S. Grand Blvd., St. Louis, MO 63104.